Solvent-Controlled Acceleration of Electron Transfer in Binary Mixtures

Audrius Pugžlys, Harald P. den Hartog, Andrius Baltuška, Maxim S. Pshenichnikov,*
Siva Umapathy,† and Douwe A. Wiersma

Ultrafast Laser and Spectroscopy Laboratory, Optical Sciences, Department of Chemistry, Materials Science Centre, University of Groningen, Nijenborgh 4, 9747 AG Groningen, The Netherlands, and Department of Inorganic and Physical Chemistry, Indian Institute of Science, Bangalore 560012, India

Received: June 21, 2001; In Final Form: October 4, 2001

We report a 5-fold acceleration of the backward intermolecular electron transfer between a rhodamine 800 dye molecule and *N,N*-dimethylaniline (DMA). This effect results from the controlled variation of the solvent dynamical properties in binary mixtures of DMA and acetonitrile. The observed acceleration reflects the competition between solvent-controlled and nonadiabatic electron transfer in the limit of barrierless reaction. A linear dependence of the electron-transfer time on the longitudinal relaxation time, as predicted by the outer sphere electron-transfer model by Rips and Jortner [Rips, I.; Jortner, J. *J. Chem. Phys.* **1987**, *87*, 2090.], is clearly observed.

1. Introduction

Electron transfer (ET) is one of the most fundamental and widespread reactions in nature and therefore has been extensively studied.[1–4] In many cases, in particular in polar solvents, solvation plays a prominent role. First, solvation changes the energy of reactants and products with respect to their energy in the gas phase. Second, solvation affects the exchange of energy and momentum among the reactants, thereby providing a drive to overcome the reaction barrier and enabling the products to dissipate their excess energy.

The majority of the ET theories is based on a dielectric continuum model in which the solvent is characterized by the macroscopic dielectric susceptibility.[3] Its spectrum includes a low-frequency part, which is well described by the Debye formula, and a high-frequency part that contains various contributions from inter- and intramolecular vibrational modes of the solvent. These two parts determine, respectively, the long-time behavior (diffusional dynamics) and the short-time behavior (inertial dynamics) of the solvent. When an ET reaction occurs on the same time scale as the solvent relaxation, the ET rate turns out to be restricted by the solvent relaxation time and the electron transfer becomes solvent controlled. When ET is faster than the solvent dynamics, the inter- and intramolecular vibrations may play an important role in governing the ET dynamics.

Marcus, in his pioneering work on ET,[4] accounted for the effect of the vastly different time scales of electronic and solvent motions on ET. Since the solvent is not able to follow the fast electronic changes during ET, the actual transfer can only take place if the solvent is in such a configuration that both product and reactant have approximately equal energies, which results in formation of a potential barrier during the ET process. Using a thermodynamic approach, Marcus derived an expression for the ET rate, which also accounts for the static properties of the solvent medium.[5]

In the early 1980s, with the advent of picosecond time resolution in spectroscopy, it was demonstrated that the dynamic

properties of the solvent can have a profound effect on the ET rate.[6] In addition, several authors pointed out that, in the case of low barrier reactions, the ET rate may not be limited by the barrier itself, but instead by the rate of the solvent response to the change in charge distribution resulting from ET.[7–10] Subsequent modifications of the theory, incorporating the influence of solvent dynamics on the ET process, showed that the inverse ET rate (τ_{ET}) is linearly proportional to the longitudinal relaxation time (τ_L) of the solvent:[7]

$$\tau_{ET} = \frac{1}{k_{ET}} = \left[\frac{(4\pi/\hbar)(V^2/E_r)}{(2\pi V^2/\hbar)(4\pi E_r kT)^{-1/2}} \tau_L + \right.$$
$$\left. \frac{1}{(2\pi V^2/\hbar)(4\pi E_r kT)^{-1/2}} \right] e^{(\Delta E - E_r)^2/4 E_r kT} \quad (1)$$

Here V is the electronic coupling, E_r is the solvent reorganization energy, and ΔE is the (free) energy gap between the reactant and the product. Parameter $E_A = (\Delta E - E_r)^2/4E_r$ in eq 1 corresponds to the height of the barrier and is called the activation energy. To make the predicted competition between the ET and dielectric relaxation more apparent, eq 1 can be recast as

$$\tau_{ET} = \tau_{ET}^{NA} + \tau_{ET}^{AD} = \tau_{ET}^{NA} + B(T)\tau_L \quad (2)$$

where τ_{ET}^{NA} and τ_{ET}^{AD} are the ET time constants in the cases of the conventional nonadiabatic limit and solvent-controlled limit, respectively, and $B(T) = (16\pi kT/E_r)^{1/2} \exp(E_A/kT)$ is a proportionality coefficient. [There is a controversy concerning the factor *4* in the eq 1. For instance, it is 2 in the paper by Garg et al.[11] The difference, despite being irrelevant to the predicted linear behavior in eq 2, may result in a different value of the solvent reorganization energy that enters the proportionality coefficient *B(T)*.] At room temperature and in the case of a small activation energy (low barrier of the reaction), the proportionality coefficient $B(T)$ has been shown to be about unity. This means that the adiabatic contribution dominates the ET dynamics for long longitudinal relaxation times.

---

* To whom correspondence should be addressed. Tel: +31.50.3634159. Fax: +31.50.3634441. E-mail: M. S.Pshenichnikov@chem.rug.nl.
† Department of Inorganic and Physical Chemistry.

The bulk of the experimental investigations on the effect of solvent dynamics on ET have focused on intramolecular ET,[2,12−15] and, more recently, on the electron donor−acceptor complexes[16−18] along with the intermolecular ET.[19−22] Solvent control of intramolecular ET has also been reported for several cases.[12] However, in the case of intramolecular ET, the relative orientation and distance of the donor and acceptor are fixed by a molecular structure. In contrast, in case of intermolecular ET the solvent has a profound influence on the geometry of the reactants. Therefore, in the latter case, the role of the solvent is expected to be more prominent as compared to intramolecular ET. With the availability of femtosecond time resolution in spectroscopy, clear violations of the solvent-controlled limit have been observed.[14,23] It has been pointed out that vibrations can play an active role in the ET process which obscures the role of the solvent.[15,18] It has also been argued by Rips and Jortner that the solvent controlled limit is not applicable to ET in the barrierless regime.[7,24]

As can be deduced from eq 2, the ET rate is determined by the longitudinal relaxation time τ_L, which is connected to the Debye relaxation time τ_D by a simple relation:[25]

$$\tau_L = \frac{n^2}{\epsilon}\tau_D \tag{3}$$

Here n and ϵ are the index of refraction and the dielectric constant, respectively. It has been shown that the Debye relaxation time is unambiguously related to longitudinal relaxation[26] and to collective orientational relaxation.[27,28] In a particular case of the Debye approximation limit $\tau_D = \tau_K$, where τ_K is the time constant of the OHD Kerr signal decay. This approximation is valid for low frequencies $\omega t_{DEBYE} \leq 1$ or when solvent friction is high, while the moment of inertia is negligibly small. In the more general case, the correction factors depending on the friction coefficient and momentum of inertia of the molecule have to be incorporated.[27,28]

Another approach to the problem of relating the OHD Kerr signal decay time to the Debye relaxation time relies on the assumption that the dynamics measured by the OHD Kerr technique originates from single-particle reorientational motion. Castner and Maroncelli[29] applying power-law relations deduced the so-called scaling exponents of 3 between the collective polarizability anisotropy correlation function and the dipole autocorrelation function. The reported relation[29] is equivalent to a scaling factor of 3 between the Debye relaxation time and the single-molecule orientational correlation time[30] in the case of insignificant inertial motion and/or collective dynamics.

In this paper we present the first experimental proof of an ET reaction whose rate can be controlled by varying the dynamical properties of the solvent. We show that a linear dependence of the inverse ET rate on the solvent longitudinal relaxation time exists as predicted by eq 1. We demonstrate that the ET reaction rate can be increased by more than a factor of 5 by the proper choice of solvent, signifying the change from solvent-controlled to nonadiabatic ET. The key virtue of the study is the use of binary mixtures, which allows a continuous variation of the relaxation properties of the solvent as has been shown recently in a study of solvation dynamics.[31]

2. Experimental Section

2.1. Materials. As a model system, Rhodamine 800 (R800) dissolved in *N,N*-dimethylaniline (DMA) electron-donating solvent was used. In most of the solvents R800 strongly fluoresces; however, in DMA the fluorescence is severely quenched. For similar systems it has been shown that the nonradiative channel, responsible for quenching, is ET that occurs from DMA to the dye molecule upon optical excitation of the latter.[23,32−34]

We have chosen acetonitrile (AN) as the second solvent in the binary mixture for the following reasons. First, AN is one of the fastest responding polar solvents[35] and is miscible with DMA in any concentration. Second, by using solvents whose static solvation properties (i.e., polarity, aproticity, etc.) are similar, while dynamic properties (such as the Debye relaxation time) are markedly different, one can clearly distinguish between solvent-dependent dynamical and equilibrium properties. Finally, the solvent dynamics of AN can be reasonably well described by a dielectric continuum model,[36] most probably because of the absence of complications associated with hydrogen bonding.

R800 (perchlorate) was purchased from Lambda Physik. DMA of the highest commercially available purity (better than 99%) and AN (HPLC far UV) were obtained from Merck and Lab-Scan, respectively, and used without further purification.

2.2. Measurement of the ET Rate. To investigate the ET process, we employed ultrafast frequency resolved pump−probe spectroscopy. In this experiment the pump pulse excites the dye molecule, initializing ET, while the delayed probe pulse monitors the photoinduced changes of population at different wavelengths. The experiments were performed using a home-built 1 kHz Ti:sapphire laser[37] and two noncollinearly pumped optical parametric amplifiers (NOPA).[38] Briefly, the laser system consists of a Ti:sapphire master oscillator pumped by an all-solid-state, diode-pumped frequency-doubled Nd:YVO₄ laser (Coherent Verdi), a pulse selector, a stretcher/compressor pair (Kapteyn-Murnane Laboratories L.L.C.), and an eight-pass Ti:sapphire amplifier pumped by a Q-switched frequency-doubled Nd:YLF laser (Quantronix 527DP−H). The laser produces 25-fs, 800-μJ pulses centered at 800 nm at 1-kHz repetition rate. After frequency doubling in a 1-mm Type I BBO crystal, two fractions of the ∼200-μJ output pulse are used to pump two NOPA's based on 2-mm, Type I BBO crystals (EKSMA Lasers, Optics, Electronics Co). Each NOPA produces ∼4-μJ, ∼30-fs pulses tunable in the 450−750-nm spectral region, which are used as the pump and the probe sources.

The sample is excited with pulses centered around the absorption peak of R800 in DMA at the wavelength of 700 nm and probed in the spectral region 670−730 nm. Since a NOPA produces pulses with a rather broad spectrum (∼60-nm fwhm at 700 nm), we use interference filters with a 10-nm bandwidth to select the wavelength of the probe pulse. This lowers the time resolution of the experiments to ∼150 fs. The pump and probe pulses after attenuation are focused into a 100-μm flow cell containing the sample. The optical density of the sample does not exceed ∼0.3 at the absorption maximum. Behind the sample, the transient absorption is measured using a photodiode and a lock-in amplifier.

Both pump and probe beams have identical polarizations. In a separate experiment, performed with orthogonal polarizations, we established that the initially induced anisotropy decays single-exponentially with a time constant of 85 ± 5 ps. Since the time scale of all relevant processes of interest is much shorter (on the order of 10 ps, vide infra) the particular choice of polarizations does not affect the measured data.

2.3. Measurement of the Longitudinal Relaxation Time. To determine solvent relaxation time constants, OHD-Kerr experiments were performed as proposed by McMorrow and Lotshaw.[39] Briefly, we used a Ti:sapphire oscillator delivering 12-fs pulses centered around 800-nm at an 82-MHz repetition

Electron Transfer in Binary Mixtures

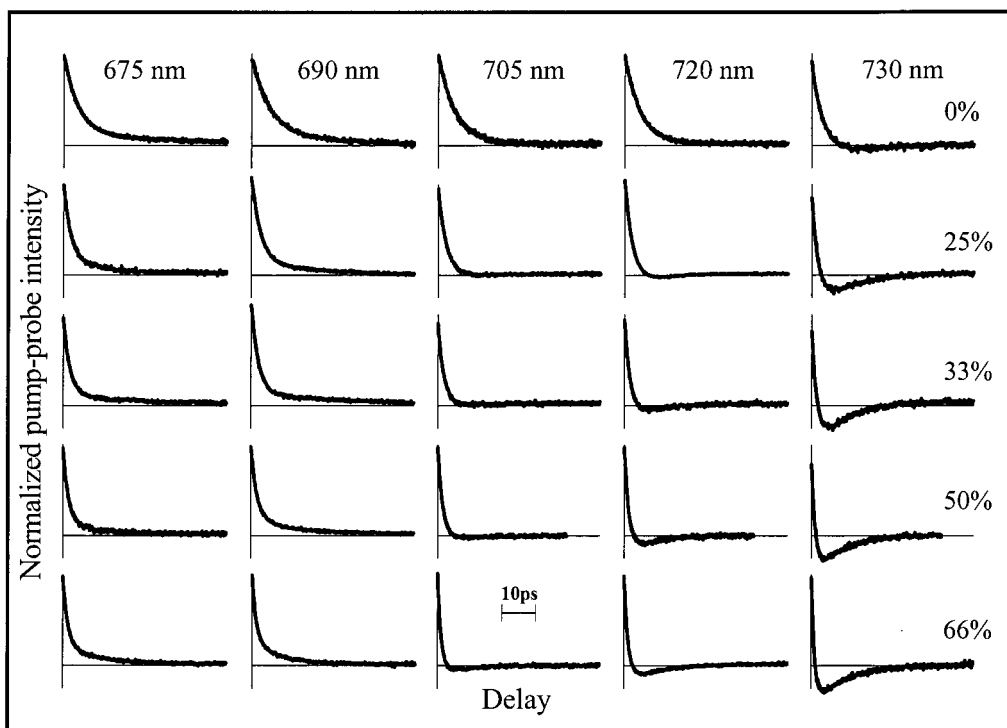*J. Phys. Chem. A, Vol. 105, No. 51, 2001* **11409**

Figure 1. Frequency-resolved pump−probe transients for R800 dissolved in AN-DMA mixtures. Columns and rows correspond, respectively, to different probe wavelengths (indicated in the upper row) and AN concentration in binary mixture (shown in the last column).

rate. The necessary pump and probe polarization orientations were set by 3-mm thick Glan-Taylor polarizers and a $\lambda/2$ plate in the pump beam. The 90° out-of-phase local oscillator field was generated by insertion of a $\lambda/4$ plate in the probe beam and detuning of the probe polarizer by ∼1.5°. The sample, i.e., the binary mixture of DMA and AN, was placed in a 200-μm standing quartz cell.

Following the arguments of Kalmykov and Quinn[27] that the effect of molecular inertia can be excluded at low frequencies, we assigned the decay time of the tails of the OHD-Kerr transients to the Debye relaxation time. The tails of the OHD-Kerr signals were fitted to a single exponent that excellently described decays in all cases. To determine the longitudinal relaxation time, we scaled the Debye relaxation time by the n^2/ϵ ratio (eq 3). The dielectric constants of binary mixtures that enter eq 3 were calculated by applying a logarithmic mixing rule[40] while the refraction indices were calculated with the local field effect taken into account.[40]

3. Results and Discussion

To investigate the ET dynamics we measured the recovery of the photoinduced bleaching at different probe wavelengths around the main maximum of the steady state absorption of R800 located around 700 nm. Photoinduced bleaching of the ground state is informative because it is sensitive to both forward and backward ET. The forward and backward ET contributes to the measured signal via depopulation of the excited state and by repopulation (recovery) of the ground state, respectively. In general, ground state recovery times are different at different wavelengths or, in other words, ground state relaxation is a continuous process with respect to the spectral evolution and cannot be represented by a single exponential process. This makes it difficult to extract the backward ET transfer rate directly from the ground-state recovery measured at a single wavelength and requires frequency resolved measurements.

In Figure 1. the kinetics representing the decay of the bleaching of the ground state at different probe wavelengths (columns) is plotted for different concentrations of AN in the binary mixture (rows). The initial decay of the bleaching (during the first 500 fs following the excitation) is dominated by the contribution of the forward ET that occurs with a time constant of $\tau_{forwardET} \sim 150$ fs.[32] This time constant is of the same order as the temporal resolution of the experiment and will not be analyzed further. The decay of the signal after ∼0.5 ps (or approximately $3\tau_{forwardET}$) is attributed to ground-state recovery caused by the backward ET. From Figure 1 one can infer that ground-state recovery dynamics has the following features: with the increase of the probe wavelength and AN fraction in the solvent, the decay of the signal shortens and the relative contribution of photoinduced absorption (negative signals) rises.

For a rigorous data analysis it is necessary to identify the processes contributing to the pump−probe signal. The positive contribution to the kinetics is caused by the bleaching of the ground state, and decays with its recovery. The negative signal, corresponding to the photoinduced absorption, can be caused by absorption of the ET state and/or the hot ground state. However, there are two observations that clearly indicate that the contribution of the former is negligibly small if any. First, in a separate experiment performed with 30-fs pump and probe pulses we have established that the bleaching signal loses approximately half of its initial amplitude after forward ET occurs (i.e., within the first 300−400 fs) without any probe wavelength dependence. This corresponds perfectly to the complete depopulation of the excited state due to forward ET and absence of the induced absorption from the ET state. The latter process would have reduced the signal below the 50%-level. This strongly suggests that the ET state is dark in the spectral region of the probe pulse (675−730 nm). Second, as it follows from Figure 1, the induced absorption is stronger at the longer wavelengths which is a clear signature of hot ground-state absorption.
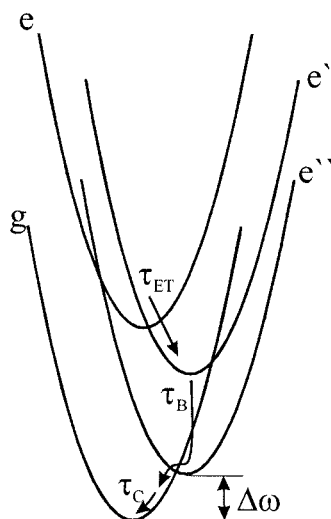
Figure 2. Schematic representation of the ultrafast dynamics in a R800−DMA/AN system after photoexcitation. g, e, e′, and e″ indicate, respectively, the potential energy surfaces of the R800 molecule in the ground state, in the excited state, in the charge-transfer state, directly after forward ET, and in the charge-transfer state just before backward ET. τ_{ET}, τ_B, and τ_C are forward ET, backward ET, and ground-state cooling time constants, while $h\Delta\omega$ designates the energy to which the backward ET occurs.

Based on the above considerations, we fitted the kinetics by applying a model which includes two processes: backward ET and cooling of the hot ground state (Figure 2). Consequently, the pump−probe signal at frequency Ω and delay time t can be described as

$$S(\Omega,t) = A_0[\sigma_0(\Omega - \omega_0) - A(t)\sigma_0(\Omega - \omega_0 - \omega(t))] \quad (4)$$

where $\sigma_0(\Omega - \omega_0)$ denotes the lineshape of the ground-state bleaching with maximum at the frequency ω_0 and A_0 is the amplitude. The first term in the eq 4 represents the initial bleaching (hole) of the ground state with amplitude while the second term describes the hot ground-state absorption with the time-dependent amplitude $A(t)$. The hot ground state is populated via the backward ET:

$$A(t) = 1 - e^{-t/\tau_B} \quad (5)$$

with τ_B being the backward ET time. Also, the absorption contour shifts toward ω_0 because of cooling of the hot ground state:

$$\omega(t) = \Delta\omega e^{-t/\tau_C} \quad (6)$$

In eq 6, $\Delta\omega$ is the initial spectral shift that shows the energy of the ground-state potential, at which the backward ET takes place, and τ_C is the cooling time constant. The line-shapes of the ground state bleaching and the hot ground state absorption were constructed numerically from the steady-state absorption spectra for different concentrations of AN in binary mixtures. A small difference in polarity of AN and DMA influences the static solvation process and causes a slight blue shift of the steady sate absorption spectra with increasing concentration of AN. To keep a minimum number of parameters in the fit procedure we assumed that the line shape of the hot ground-state absorption remains unchanged.

After the estimation of τ_C and ω_0 from the steady state absorption spectra, the data depicted in Figure 1 were fitted globally by varying parameters A_0, $\Delta\omega$, and τ_B. Representative fits shown in Figure 3a,b clearly demonstrate the success of the model. The results of the fitting are listed in Table 1.
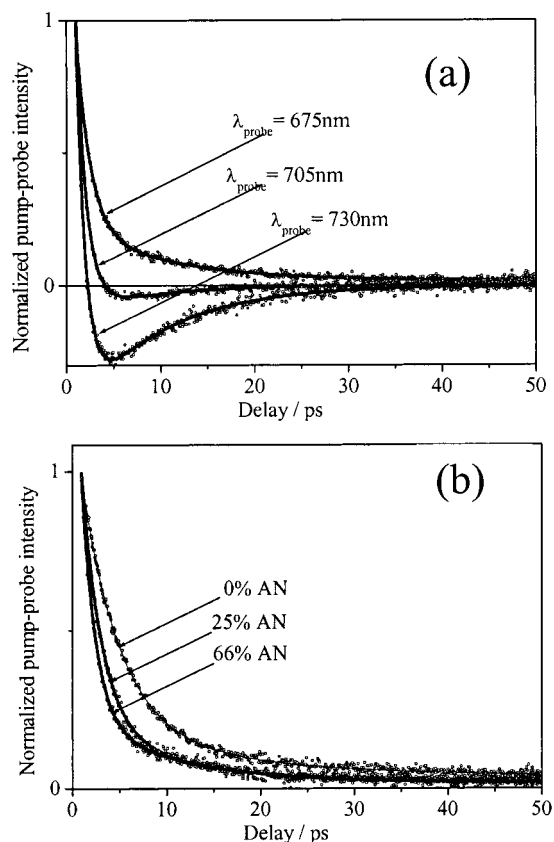

Figure 3. Experimental data (open circles) and fits (solid curves) for different probe wavelengths in the case of 66% of AN−DMA mixtures (a) and for different concentrations of AN in binary mixture at probe wavelength 675 nm (b). The fit parameters are given in Table 1.

TABLE 1: Results of the Fitting of Frequency-Resolved Pump−Probe Transients by Applying the Model Presented by Equations 4−6[a]

C_{AN}/%	$\Delta\omega$/cm^{-1}	τ_B/ps	τ_C/ps
0	70 ± 27	4.7 ± 0.7	8.4 ± 0.6
25	80 ± 20	2.5 ± 0.4	8.3 ± 2.0
33	61 ± 28	1.9 ± 0.2	8.0 ± 1.1
50	60 ± 30	1.6 ± 0.2	8.4 ± 1.5
66	70 ± 20	1.2 ± 0.2	8.5 ± 1.1
summary	70 ± 30	f(C_{AN})	8.3 ± 2.0

[a] C_{AN} is the volume percentage of AN in the binary mixture, $\Delta\omega$ is the initial spectral shift of the hot ground-state potential, and τ_C and τ_B are the cooling and the backward ET time constants, respectively.

Clearly, backward ET demonstrates a remarkable sensitivity to the AN content. For instance, in a 75/25% DMA/AN mixture, the backward ET time decreases to ∼2.5 ps (from ∼4.5 ps in the case of pure DMA) while for the 50/50% mixture the acceleration is even greater. Finally, the decay time reaches its lowest value of ∼1.2 ps in a mixture containing 66% AN. The pump−probe signal obtained for R800 in pure AN does not exhibit any substantial decay in the time window of the experiment, which is fully consistent with the absence of an ET process.

Figure 4 summarizes the obtained results on the backward ET time, which monotonically decreases with the increase of the AN content in the DMA/AN binary mixture. To verify the conclusion that ET acceleration is directly connected to the change of the solvent dynamical properties, we substituted AN with benzonitrile (BN). It has been shown that solvation dynamics in BN is nearly 20 times slower than in AN[35] while the dipole moments and solvatiochromic polarity[41,42] of both

Electron Transfer in Binary Mixtures

J. Phys. Chem. A, Vol. 105, No. 51, 2001 **11411**
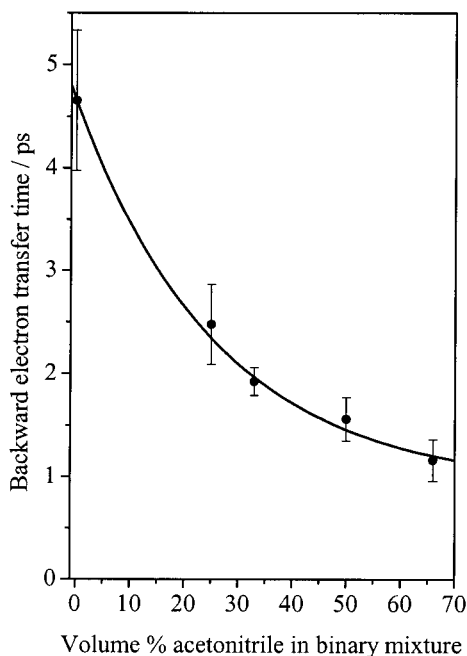

Figure 4. The dependence of the backward ET time in R800−DMA/AN system on the volume percentage of AN in AN−DMA mixtures. The solid line is meant as a guide for the eye.

Figure 5. The solvent rotational diffusion time as a function of the volume percentage of AN in a AN−DMA mixtures. The linear fit to the data is shown by the solid line. In the insert, OHD Kerr transients of pure DMA (top curve), 50/50% mixture of DMA/AN (middle curve), and pure AN (bottom curve) are shown. Bold lines represent single-exponential fits of the tails of the transients.

solvents are similar enough to expect comparable solvation dynamics if static properties of solvent were to play a major role. As expected, no acceleration of the backward ET was observed in mixtures of DMA and BN.

Solvent polarity can influence the rate of an ET reaction by affecting solvation in a static and dynamic manner by changing the energy of reactants and products with respect to their energy in the gas phase, and by influencing the exchange of energy and momentum among the reactants. The dipole moments of DMA (1.68 D) and AN (3.92 D) are sufficiently different to influence−at least potentially−the ET rate. On the other hand, the dipole moment of AN is smaller than one of BN (4.18 D) and the polarizability of BN is nearly three times larger than that of AN. Therefore, the influence of the static polarity on ET rate, if such were to exist, is expected to be more pronounced in the case of a BN/DMA binary mixture. No such influence has been observed which strongly suggests that a static solvent polarity does not affect appreciably the rate of ET reaction. In contrast, dynamical solvation together with vibrational cooling is responsible for the lowering of the energy of the product in the ET state which is directly related to the dynamical properties of solvent molecules.

After backward ET is completed, the hot ground state has only $\sim$70 cm^{-1} excess vibrational energy, which is substantially less than the kT value at room temperature ($\sim$200 cm^{-1}). This provides evidence that the energy of the product (ET state) just before the backward ET takes place, is practically at the bottom of the ground-state of the reactant (equilibrated R800 molecule). The very small difference between the energies of the product and reactant suggests that backward ET is a nearly barrierless process.

The last comment on the applied model concerns cooling of the ground state. It occurs with a time constant of $\sim$8 ps that does not depend on the AN concentration. This could be explained by taking into account the fact that the cooling process involves relaxation of both intra- and intermolecular modes. Consequently, in the case of a "very fast" solvent, the cooling is mainly determined by the speed of the internal vibrational
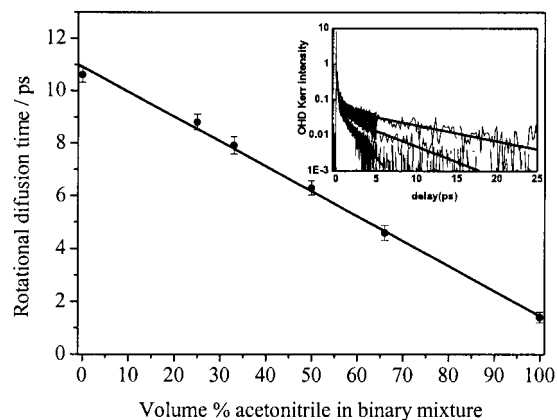
relaxation of a solute molecule. In this case, the excess vibrational energy is transferred from the solute to the solvent almost instantaneously, and the speed of intramolecular relaxation becomes the limiting factor in the cooling process. Recently Xu et al.[22] applied the techniques of transient grating and photon echo spectroscopy to study intermolecular ET dynamics in the rhodamine 6G−DMA system. They reported time constants for backward ET and hot ground-state recovery as 4.0 and 19 ps, respectively. The former value is in excellent agreement with our result obtained for neat DMA (4.5 ps). Some discrepancy in time constants of the relaxation of the hot ground state is consistent with the assumption of the intramolecular nature of the cooling process and different spectral density of the intramolecular modes in the case of Rhodamine 6G and R800 molecules.

In Figure 5 the rotational diffusion time determined from transients measured in the OHD Kerr experiment (Figure 5, inset), is presented as a function of the volume percentage of AN in the mixture. The value of $\sim$11.5 ps for pure DMA corresponds to the amplitude-weighed average of the two decay components found by Meech and co-workers,[43] while the decay of $\sim$1.3 ps for pure AN agrees very well with the one reported by McMorrow and Lotshaw.[44] The relaxation times of binary mixtures show a linear dependence on the AN concentration. This is fully consistent with the fact that the rotational relaxation time depends on the bulk parameters of the solvent (i.e., viscosity and density) which vary almost linearly with the concentration of the components.[45]

In Figure 6 the backward ET time, as extracted from the pump−probe kinetics (Figure 4), is plotted against the solvent longitudinal relaxation time calculated from the rotational diffusion time according to eq 3. A linear dependence of the ET time on the longitudinal relaxation time as predicted by the outersphere ET model[7,24] (see eq 1) is clearly observed. The slope of the linear fit to the experimental points amounts to 0.7 $\pm$ 0.1 and corresponds to the proportionality coefficient $B(T)$ in eq 2, while an extrapolation of the straight line in Figure 6 to $\tau_D = 0$ ps shows that in the case of conventional nonadiabatic limit (i.e, in an infinitely fast solvent) the backward ET time would be $\tau_{ET}^{NA} = 0.7 \pm 0.1$ ps. According to eq 1, the backward ET time τ_{ET}^{NA} is inversely proportional to the square of the value of the electronic coupling V between donor and acceptor (in the case of the conventional nonadiabatic limit). However, the electronic coupling at very low concentrations of DMA may
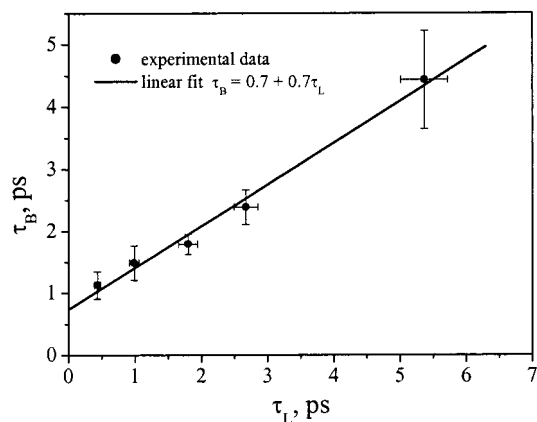
11412 *J. Phys. Chem. A, Vol. 105, No. 51, 2001*

Pugžlys et al.

Figure 6. The backward ET time τ_B as a function of the longitudinal relaxation time τ_L. The linear fit $\tau_B = \alpha + \beta\tau_L$ to the experimental data (solid circles) is shown by the solid line. The fit parameters are $\alpha = 0.7 \pm 0.1$ and $\beta = 0.7 \pm 0.1$ ps.

become diffusion-dependent. Therefore, some deviations from a linear dependence of ET time constant on the longitudinal relaxation time are expected in this case. None have been observed, however, in our experiments down to 30% DMA concentration.

In the case of pure DMA as a solvent, the inequality $\tau_{ET}^{NA} \ll \tau_{ET}^{AD}$ holds, and therefore, the solvent relaxation is the predominant rate-limiting process for the intermolecular backward ET reaction. In contrast, in the case of 66% of acetonitrile in the binary mixture, the nonadiabatic term dominates ($\tau_{ET}^{NA} \gg \tau_{ET}^{AD}$), i.e., the ET rate becomes mainly determined by the electronic coupling between donor and acceptor. In the case when AN concentration in the binary mixture is less than 66% the competition between the ET and the dielectric relaxation takes place. In particular, these two processes become as important in a mixture containing equal amounts of DMA and AN, when $\tau_{ET}^{NA} \cong \tau_{ET}^{AD}$. The slope of 0.7 corresponding to the proportionality coefficient *B(T)* in eq 2, reveals that at room temperature and in the case of barierless transition ($E_A \ll kT$) the reorganization energy of the solvent E_r is in the order of $10\,000$ cm^{-1} (see footnote in the Introduction). This value is in a perfect agreement with the one predicted by the theory of outer sphere ET.[21]

It has been pointed out by Lyndel-Bell[30] and Castner[29] that a scaling factor of 3 is required between the Debye relaxation time and a single-molecule orientational correlation time to account for possible intermolecular correlations. Although the linear weighing of τ_L with respect to τ_K does not change the linear dependence of the backward ET time on the longitudinal relaxation time, it might affect the proportionality coefficient *B(T)* (eq 2) along with the values of τ_{ET}^{NA} and E_r. However, according to the data presented by Castner and Maroncelli[29] the scaling factor of 3 holds only for AN but not for DMA. Consequently, the scaling of the time constant of the OHD Kerr signal decay by a factor of 3 for AN at the time when a factor of 1 holds for DMA makes the linear dependence (Figure 6) only slightly steeper leading to a minor change in the values of τ_{ET}^{NA} and E_r.

In conclusion, by utilizing the technique of binary mixtures of DMA and AN, we have been able to speed up the backward ET between R800 and DMA by a factor of 5. The acceleration is well described by the outersphere electron transfer models, using the dielectric relaxation time obtained by the OHD-Kerr technique. We have also shown that the observed acceleration corresponds to the continuous change from solvent-controlled

to nonadiabatic ET in the limiting case of barrierless intermolecular ET. Our results demonstrate that the backward ET in R800-DMA system is accomplished practically to the bottom of the ground state, i.e., the potential surface of the product before backward ET takes place is already lowered nearly to the level of the bottom of the ground-state potential of the reactant. This indicates a very small potential energy barrier in the case of backward ET.

The obtained results on ET transfer rate in binary mixtures raise an intriguing question on whether the forward ET can be accelerated in binary mixtures of solvents that show inertial solvent reorganization on markedly different time scales. Although our data are not conclusive yet, we have indeed observed the increase in the forward ET rate with the increase of AN concentration. The integrated pump−probe experiments with 18-fs pulses centered around 700 nm allowed us to resolve the initial 150-fs component which is caused by the depletion of the excited-state population due to forward ET.[46] The value of 150-fs corroborates with the ET time scales reported for similar dye molecules dissolved in DMA.[22,23,32−34] The preliminary data show that the forward ET process speeds up by a factor of 2 as a result of an increase in the AN content in the binary mixture up to 75%. It has been pointed out by Northrup and Hynes[47] that, in order to influence the rate of a chemical reaction, solvent dynamics should take place on the time scale of the crossing of the "barrier-top region". For R800 dissolved in DMA/AN mixtures, this implies that mainly the initial inertial solvent dynamics should affect the rate of forward ET. A detailed discussion on forward ET in R800 dissolved in DMA/AN mixtures will be presented elsewhere.

References and Notes

(1) Marcus, R. A.; Sutin, N. *Biophys. Biochem. Acta* **1985**, *811*, 265.
(2) Barbara, P.; Meyer, T.; Ratner, M. *J. Phys. Chem.* **1996**, *100*, 13148.
(3) Hsu, C.-P.; Song, X.; Marcus, R. A. *J. Phys. Chem. B* **1997**, *101*, 2546.
(4) Marcus, R. A. *J. Chem. Phys.* **1956**, *24*, 966.
(5) Marcus, R. A. *Annu. Rew. Phys. Chem.* **1964**, *15*, 155.
(6) Kosower, E. M.; Huppert, D. *Chem. Phys. Lett.* **1983**, *96*, 433.
(7) Rips, I.; Jortner, J. *J. Chem. Phys.* **1987**, *87*, 2090.
(8) Hynes, J. T. *J. Phys. Chem.* **1986**, *90*, 3701.
(9) Sumi, H.; Marcus, R. A. *J. Chem. Phys.* **1986**, *84*, 4894.
(10) Zusman, L. D. *Chem. Phys.* **1980**, *49*, 295.
(11) Garg, A.; Onuchic, J. N.; Ambegaokar, V. *J. Chem. Phys.* **1985**, *83*, 4491.
(12) Zijlstra, R. W. J.; Duijnen, P. T. v.; Feringa, B. L.; Steffen, T.; Duppen, K.; Wiersma, D. A. *J. Phys. Chem. A* **1997**, *101*, 982.
(13) Masad, A.; Hupert, D.; Kosower, E. M. *Chem. Phys.* **1990**, *144*, 391.
(14) Akesson, E.; Walker, G. C.; Barbara, P. F. *J. Chem. Phys.* **1991**, *95*, 4188.
(15) Barbara, P. F.; Walker, G. C.; Smith, T. P. *Sience* **1992**, *256*, 975.
(16) Kimura, Y.; Takebayashi, Y.; Hirota, N. *J. Chem. Phys.* **1998**, *108*, 1485.
(17) Wynne, K.; Gali, C.; Hochstrasser, R. M. *J. Chem. Phys.* **1994**, *100*, 4797.
(18) Wynne, K.; Reid, G. D.; Hochstrasser, R. M. *J. Chem. Phys.* **1996**, *105*, 2287.
(19) Yoshihara, K.; Tominaga, K.; Nagasawa, Y. *Bull. Chem. Soc. Jpn.* **1995**, *68*, 696.
(20) Castner, E. W.; Jr., D. K.; Cave, R. J. *J. Phys. Chem. A* **2000**, *104*, 2869.
(21) Pal, H.; Shirota, H.; Tominaga, K.; Yoshihara, K. *J. Chem. Phys.* **1999**, *110*, 11454.
(22) Xu, Q.-H.; Scholes, G. D.; Yang, M.; Fleming, G. R. *J. Phys. Chem. A* **1999**, *103*, 10348.
(23) Kobayashi, T.; Takagi, Y.; Kandori, H.; Kemnitz, K.; Yoshihara, K. *Chem. Phys. Lett.* **1991**, *180*, 416.

(24) Bixon, M.; Jortner, J. *Chem. Phys.* **1993**, *176*, 467.

(25) Friedman, H. *J. Chem. Soc., Faraday Trans. 2* **1983**, *79*, 1465.

(26) Kivelson, D.; Friedman, H. *J. Phys. Chem.* **1989**, *93*, 7026.

(27) Kalmykov, Y. P.; Quinn, K. P. *J. Chem. Phys.* **1991**, *95*, 9142.

(28) Coffey, W. T.; Dejardin, J.-L.; Kalmykov, Y. P.; Quinn, K. P. *Chem. Phys.* **1992**, *164*, 357.

(29) E. W. Castner, J.; Maroncelli, M. *J. Mol. Liq.* **1998**, *77*, 1.

(30) Lynden-Bell, R. M.; McDonald, I. R. *Mol. Phys.* **1981**, *43*, 1429.

(31) Gardecki, J. A.; Maroncelli, M. *Chem. Phys. Lett.* **1999**, *301*, 571.

(32) Kandori, H.; Kemnitz, K.; Yoshihara, K. *J. Phys. Chem.* **1992**, *96*, 8042.

(33) Yartsev, A. P.; Nagasawa, Y.; Douhal, A.; Yoshihara, K. *Chem. Phys. Lett.* **1993**, *207*, 546.

(34) Seel, M.; Engleiter, S.; Zinth, W. *Chem. Phys. Lett.* **1997**, *275*, 363.

(35) Horng, M.-L.; Gardecki, J. A.; Maroncelli, M. *J. Phys. Chem. A* **1997**, *101*, 1030.

(36) Yarzeba, W.; Walker, G. C.; Johnson, A. E.; Barbara, P. F. *Chem. Phys.* **1991**, *152*, 57.

(37) C. G. Durfee, I.; Backus, S.; Murnane, M. M.; Kapteyn, H. C. *IEEE J. Quantum Electron.* **1998**, *4*, 395.

(38) Wilhelm, T.; Piel, J.; Riedle, E. *Opt. Lett.* **1997**, *22*, 1494.

(39) McMorrow, D.; Lotshaw, W. T.; Kenney-Wallace, W. T. *IEEE J. Quantum Electron.* **1988**, *QE−24*, 443.

(40) Condon, E. U.; Odishaw, H. *Handbook of physics*, second ed.; McGraw-Hill Book Company:, 1967.

(41) Laurence, C.; Nicolet, P.; Dalati, M. T.; Abboud, J.-L. M.; Notario, R. *J. Phys. Chem.* **1994**, *98*, 5807.

(42) Reichardt, C. *Chem. Rev.* **1994**, *94*, 2319.

(43) Smith, N. A.; Lin, S.; Meech, S. R.; Shirota, H.; Yoshihara, K. *J. Phys. Chem. A* **1997**, *101*, 9578.

(44) McMorrow, D.; Lotshaw, W. T. *J. Phys. Chem.* **1991**, *95*, 10395.

(45) Kivelson, D. *Rotational Dynamics of Small Molecules and Macromolecule*; Springer: Berlin, 1987.

(46) Baltuska, A.; Hartog, H. d.; Pshenichnikov, M. S.; Wiersma, D. A. Unpublished.

(47) Northrup, S. H.; Hynes, J. T. *J. Chem. Phys.* **1980**, *73*, 2707.